Synthesis, Structural Characterization and Photophysical Properties of *Bis*(4′-chloro-2,2′:6′,2″-terpyridyl)nickel(II)chloride Dihydrate

B. Thippeswamy[1,2], P.A. Suchetan[1], G.R. Vijayakumar[1,*], B. Somashekara[3] and I. Mallikarjuna[2]

[1]Department of Chemistry, University College of Science, Tumkur University, Tumakuru-572103, India
[2]Department of Chemistry, Maharani's Science College for Women (Autonomous), Mysuru-570005, India
[3]Department of Chemistry, Smt. Indira Gandhi Government First Grade Women's College, Sagar-577401, India

*Corresponding author: E-mail: vijaykumargr18@gmail.com

Nickel(II) complex *viz. bis*(4′-chloro-2,2′:6′,2″-terpyridyl)nickel(II)chloride dihydrate, [Ni(Cltpy)$_2$]Cl$_2$·2H$_2$O where Cltpy is a tridentate ligand was synthesized under mild conditions by conventional method. The octahedral geometry of nickel(II) complex was revealed by single crystal X-ray diffraction (SCXRD) studies. The synthesized Ni(II) complex was characterized by Fourier transform-infrared (FT-IR), elemental analysis, scanning electron microscope (SEM), thermal analysis (TG-DTA), photoluminescence (PL) and diffuse reflectance (DR) spectra. A prominent peak at 630 nm was recorded in the DR spectrum and the band gap energy of 2.38 eV was resulted in accordance with Kubelka-Munk (K-M) theory. The photoluminescent spectra of the synthesized nickel(II) complex displayed the emission of blue green light. The commission internationale de l'eclairage (CIE) coordinates (0.2641, 0.3722) were obtained from its CIE graph.

Keywords: Terpyridine, Photoluminescence, Diffuse reflectance, Single crystal XRD, Thermogravimetry.

INTRODUCTION

Organic light emitting diode (OLED), a solid-state device, is a LED in which the emissive electroluminescent layer is an organic compound film that emits light by responding to electric current. After the successful discovery of first OLED by Tang & VanSlyke [1] with efficient characteristics, the fabrication of light emitting devices purely based on organic ligands has gathered considerable attention on account of their ability to replace customary light sources and displays [2].

In subsequent years, a considerable number of reports illustrated the use of organic ligand based metal complexes in OLED applications and in solar cells as electron transfer mediators by studying their photoluminescent properties [3-5]. Previous report demonstrated the synthesis of green light emitting *bis*(1[(4-butylphenyl)imino]methylnaphthalen-2-ol)-Ni(II) complex by investigating its crystal structure and photoluminescent properties [6] is worth mentioning. Since stable complexes are resulted from d^8 transition metal ions with chelating organic ligands, their synthesis with a special focus on exploring their thermal and luminescent properties

assumes a greater practical significance [7]. The nature of organic molecules or ligands to be incorporated in the complexes plays an important role in exhibiting light emitting properties of the material [8-11]. The planarity that establishes direct relationship with the conjugation of aromatic ligand molecules facilitates the movement of electrons and the metal complexes formed as a result of coordination of planar ligand molecules with metal ions normally gain higher stability. There are reports on the synthesis of metal complexes containing such ligands and are employed as an efficient hole transporting materials in OLEDs [12]. In this regard, nitrogen containing heterocycles, *viz.* pyridine, bipyridine, terpyridine, imidazole and other similar molecules have become promising ligands and the synthesis of such ligand containing transition metal complexes has been taken place so as to investigate their photoluminescent properties [13-15]. It was emphasized that substituents on bipyridine ring have an impact on the self-quenching of the excited state behaviour of the material and, therefore, substituted bipyridine ligands have been widely preferred over the unsubstituted ones for coordination with metal ions. Rudmann *et al.* [16] designed and synthesized derivatives of Ru(bpy)$_3^{2+}$ in an attempt to prevent

self-quenching of the excited state by incorporating different alkyl substituents on bipyridyl ligand and the devices fabricated from new Ru(bpy)$_3^{2+}$ complexes exhibited higher photoluminescence and electroluminescence efficiency than devices purely made from Ru(bpy)$_3^{2+}$.

In view of the practical applications based on the above reported complexes, a Ni(II) complex with 4′-chloro-2,2′:6′,2″-terpyridine (Cltpy) ligand was synthesized and characterized with a prime objective of examining its photophysical properties through photoluminescence and diffuse reflectance spectra. The molecular structure of the Ni(II) complex was established from its single crystal XRD data.

EXPERIMENTAL

Commercial samples of chemicals and reagents purchased from Sigma-Aldrich were used for the synthesis. The solvents were of reagent grade and employed in the synthetic process without further purification. The Fourier transform-infrared (FT-IR) spectrum was recorded by adopting scan method in the range 4000-500 cm^{-1} using Thermo-Nicolet, Avatar 370 FT-IR spectrometer by KBr pellet technique. Simultaneous thermogravimetry differential thermal analysis (TG-DTA) analyses were performed using Perkin-Elmer Pyris Diamond DSC instrument. Percentages of elements C, H and N were determined by Elementar Vario EL III analyzer. The diffuse reflectance (DR) spectrum was recorded on a Perkin-Elmer UV-visible spectrophotometer Lambda-35 and the recording of photoluminescence (PL) excitation and emission spectra was done by using spectroflourimeter, Moriba equipped with 450 W xenon lamp as an excitation source. The scanning electron microscope (SEM) images were obtained using JEOL Model JSM-6390LV.

The intensity data of synthesized Ni(Cltpy)$_2$(Cl)$_2$·2H$_2$O complex were collected on a Bruker Smart X2S diffractometer equipped with a fine focus, 3 kW sealed X-ray source (graphite monochromated Mo$K\alpha$, $\lambda = 0.71073$ Å) at 296(2) K. Image processing and data reduction were performed using SAINT-Plus and XPREP [17]. The structures were solved by direct methods using SHELXS-97 [18] within the WinGX suite [19]. The H atoms of the OH groups were located from difference maps and refined with the bond length restraint N–H = 0.82(2) Å. The C$_{arm}$ bound H atoms were positioned with idealized geometry using a riding model with C-H = 0.93Å and U$_{iso}$ = 1.2U$_{eq}$ (C$_{arm}$). In the final stages of the refinement, the analysis of data with the TWINROTMAT routine in PLATON [20] indicated the presence of a minor twin component. The structure was thus refined as a two-component inversion twin with a 0.8:0.2 domain ratio. The twin law was (-100/0-10/00-1). The molecular and packing diagrams were generated using the software MERCURY [21].

Synthesis of *bis*(4′-chloro-2,2′:6′,2″-terpyridyl)nickel(II) chloride dihydrate: A solution of 4′-chloro-2,2′:6′,2″-terpyridine (0.535 g, 2 mmol) in 5 mL ethanol was stirred on a magnetic stirrer for 0.5 h at 50 ºC and added a solution of NiCl$_2$·6H$_2$O (0.237 g, 1 mmol) dissolved in 5 mL ethanol. The reaction mixture was allowed to stir for 2 h at the same temperature and the resulting brown solution was evaporated slowly to afford brown powdered form of the Ni(II) complex. The solid product obtained was purified by trituration with toluene and then placed in a desiccator to achieve the constant weight (**Scheme-I**). Yield: 87.5%. Methanol-chloroform (1:9) solvent system was found suitable to grow brown prismatic type of crystals for SCXRD analysis. m.p. > 250 ºC. Elemental analysis of C$_{30}$H$_{24}$N$_6$O$_2$Cl$_4$Ni, calcd. (found) %: C, 51.40 (50.24); H, 3.45 (3.39); N, 11.99 (11.62); Ni, 8.37 (8.25). FT-IR (KBr, v_{max}, cm^{-1}): 3427.3 (OH *str.*), 3043.2 (CH arom.), 1592.5 (C=C arom.), 1413.9-1560.4 (C=N arom.), 740.9 cm^{-1} (C-Cl bend.) 414.2 (symmetric Ni-N bend.) and 493.6 (asymmetric Ni-N bend.).

RESULTS AND DISCUSSION

The complex Ni(Cltpy)$_2$(Cl)$_2$·2H$_2$O was synthesized by reacting an alcoholic solution of one equivalent of NiCl$_2$·6H$_2$O with a previously stirred alcoholic solution of two equivalents of Cltpy. The nickel(II) complex was recovered from the resulting alcoholic solution on slow evaporation. Methanol-chloroform (1:9) solvent system was found suitable to grow brown prismatic type of crystals of the nickel(II) complex for SCXRD analysis. The paramagnetic nature of the aforementioned complex was practically established, as no prominent
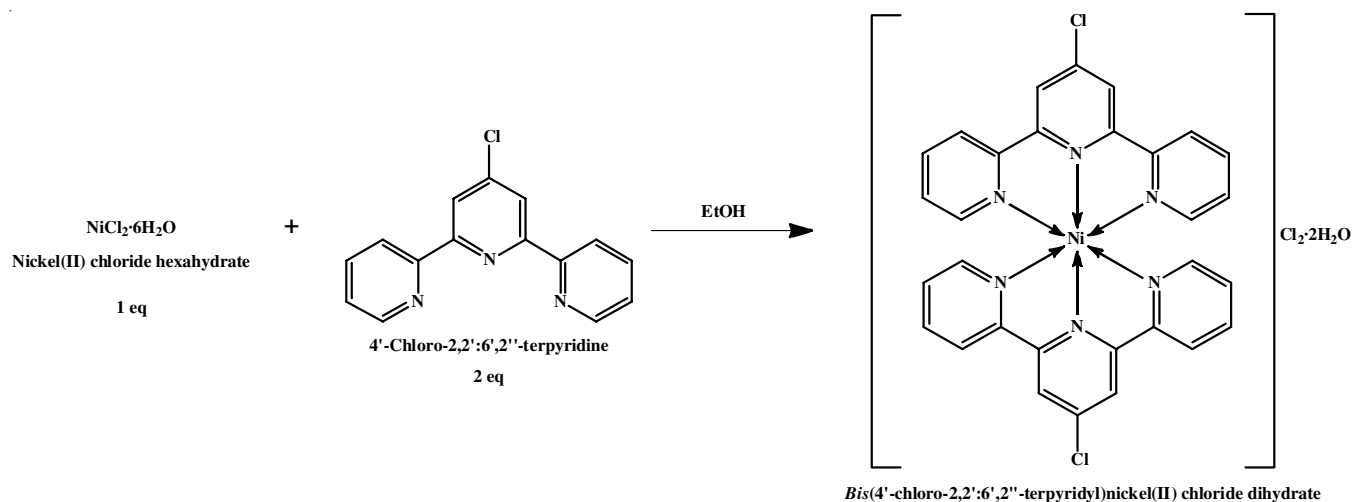
Scheme-I: Synthesis of *bis*(4′-chloro-2,2′:6′,2″-terpyridyl)nickel(II)chloride dihydrate, [Ni(Cltpy)$_2$]Cl$_2$·2H$_2$O

peak pertaining to aromatic protons was observed in its ^{1}H NMR spectrum. To substantiate our claim to according paramagnetic status of the title complex, similar complexes were also reported to exhibit paramagnetic behaviour and were not characterized by ^{1}H NMR technique [22]. The formation of nickel(II) complex, confirmed primarily by the change in colour during the course of reaction, was further established by its FT-IR spectral characterization. The shift of absorption bands in the FT-IR spectrum of the complex when compared with that of free ligand (Fig. 1) was observed.
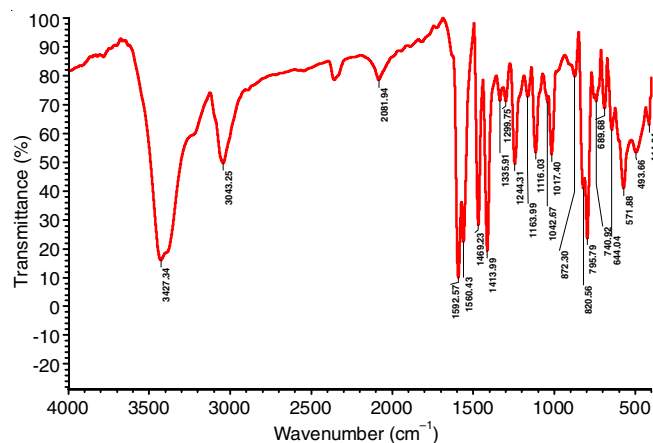

Fig. 1. FT-IR spectrum of *bis*(4′-chloro-2,2′:6′,2″-terpyridyl)nickel(II) chloride dihydrate

FT-IR spectrum of $Ni(Cltpy)_2(Cl_2)\cdot 2H_2O$ clearly indicated the presence of metal ligand bond and functional groups. The FT-IR data of the complex were found to be 3043.25 cm^{-1} (CH arom.), 1592.57 cm^{-1} (C=N arom.), 1560.43-1413.99 cm^{-1} (C=C arom.), 740.92 cm^{-1} (C-Cl bend.) 414.24 cm^{-1} and 493.66 cm^{-1} (Ni-N symmetric and asymmetric bending, respectively). The appearance of a broad band near 3427.34 cm^{-1} can be ascribed to ν(O–H) vibrations. The $[Ni(Cltpy)_2]Cl_2\cdot 2H_2O$ complex had been subjected to elemental analysis and the calculated values were correlated with the found values. The Ni(II) complex, possessing two molecules of water of hydration, was confirmed from the elemental analysis.

Thermal studies: In order to investigate the thermal properties of $[Ni(Cltpy)_2]Cl_2\cdot 2H_2O$, simultaneous measurements using TG-DTA were performed. The results of thermal analysis, summarized in Table-1, indicated good correlation between the calculated and the experimental mass loss values. However, Ni(II) complex suffers progressive decomposition in different ways. The first step resulted in the mass loss due to elimination of two water molecules in the temperature range 60-165 ℃ with an estimated mass loss of 5.05% (calcd. mass loss 5.13%). The above mass loss was evident from the appearance of an endothermic DTG peak at 161.14 ℃ (Fig. 2). The mass loss
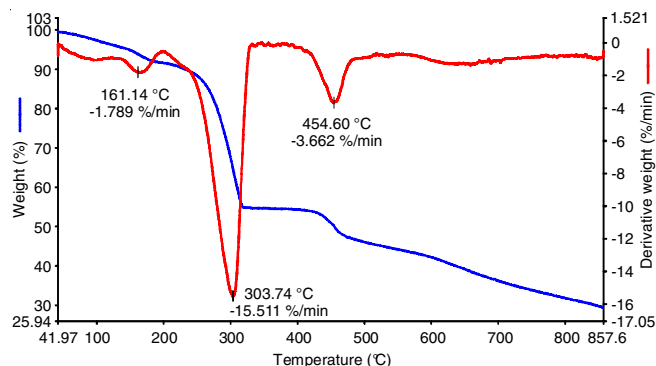

Fig. 2. TG-DTA of *bis*(4′-chloro-2,2′:6′,2″-terpyridyl)nickel(II)chloride dihydrate

that occurred in the second step was mainly ascribed to the loss of one Cltpy ligand with an estimated mass loss of 39.5% (calcd. mass loss 40.25%). The mass loss indicated in the above step was accompanied by an endothermic DTG peak at 303.74 ℃. Between 420-470 ℃, the intermediate compound obtained started to lose remaining Cltpy with the appearance of an exothermic DTG peak at 454.60 ℃ and the formation of a mixture of NiO and Ni (molar ratio 1:1) was believed to be taken place [23]. It was reported earlier that hydrated $NiCl_2$ is found to be stable up to 400 ℃, above which it suffers decomposition in the presence of inert atmosphere by dehydrochlorination, dechlorination and partial oxidation [24].

Molecular and crystal structure: The synthesized complex $Ni(Cltpy)_2(Cl_2)\cdot 2H_2O$ crystallizes with two molecules of solvent water molecule and two free chloride anions as counter ions (Fig. 3). The complex crystallizes in orthorhombic $Pna2_1$ space
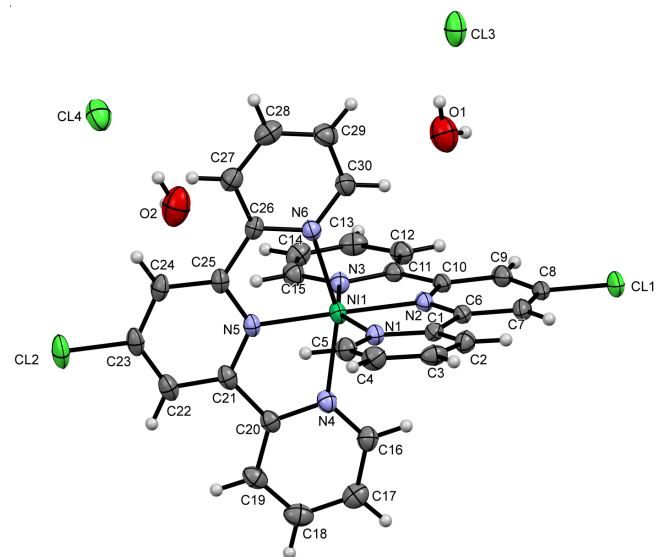
Fig. 3. An ORTEP view of $[Ni(Cltpy)_2]Cl_2\cdot 2H_2O$ with thermal ellipsoid plots drawn at 30% probability level

TABLE-1						
THERMAL DECOMPOSITION DATA FOR $[Ni(Cltpy)_2]Cl_2\cdot 2H_2O$						
Complex formula	Temperature range (°C)	DTA peak (°C)	Mass loss (%)		Intermediate and residue
			Found	Calculated	
$[Ni(Cltpy)_2]Cl_2\cdot 2H_2O$	60-165	161.14 endo	5.05	5.13	$Ni(Cltpy)_2Cl_2$
	200-320	303.74 endo	39.5	40.25	$Ni(Cltpy)Cl_2$

group. All the Ni–N coordinative bond lengths are in the range of 2.009(3)–2.116(4) Å. The complex shows deviation from the perfect octahedral geometry, with the bond angles of N4-Ni-N6 [155.63 (14)°], N2-Ni-N5 [178.92 (19)°] and N1-Ni-N3 [155.22 (14)°] deviating from ideal value of 180° (Tables 2 and 3). The two ligands are almost planar with the root mean squared deviations of all the non-hydrogen atoms being 0.052 and 0.070 Å. Further, the dihedral angle between the two ligands is 86.4°.

In crystal structure, O–H···Cl⁻ hydrogen bonds between the chloride ions and water molecules run into infinite parallel one dimensional chains running down the a axis. The complex ions are connected to these infinite chains forming pendants *via* C–H···O$_{water}$ interactions forming a two dimensional sheet along the ab-plane (Fig. 4).

The adjacent two dimensional networks are further connected along *c*-axis *via* several C-H···Cl⁻ interactions to form a three dimensional channel like network, the channel being

TABLE-2
GEOMETRIC PARAMETERS (Å, °) OF [Ni(Cltpy)₂]Cl₂·2H₂O

NI1–N5	2.009 (3)	NI1–N1–C1–C2	176.5 (4)	C15–N3–C11	117.9 (5)
NI1–N2	2.012 (3)	C5–N1–C1–C6	-178.6 (4)	C15–N3–NI1	127.1 (3)
NI1–N3	2.109 (4)	NI1–N1–C1–C6	-1.0 (5)	C11–N3–NI1	115.0 (3)
NI1–N4	2.111 (5)	N2–C6–C1–N1	3.1 (6)	C16–N4–C20	117.5 (5)
NI1–N6	2.116 (4)	C7–C6–C1–N1	-178.0 (4)	C16–N4–NI1	127.7 (4)
NI1–N1	2.113 (4)	N2–C6–C1–C2	-174.3 (4)	C20–N4–NI1	114.8 (3)
CL1–C8	1.731 (4)	C7–C6–C1–C2	4.6 (7)	C30–N6–C26	118.4 (5)
CL2–C23	1.738 (5)	C6–N2–C10–C9	-0.1 (7)	C30–N6–NI1	127.2 (4)
N2–C6	1.334 (6)	NI1–N2–C10–C9	-178.6 (3)	C14–C13–C12	119.7 (5)
N2–C10	1.347 (6)	C6–N2–C10–C11	179.1 (4)	C17–C18–C19	119.0 (5)
N5–C25	1.342 (6)	NI1–N2–C10–C11	0.6 (5)	C7–C6–C1	125.6 (4)
N5–C21	1.346 (6)	N3–C11–C10–N2	-0.3 (6)	C23–C24–C25	117.4 (5)
N1–C5	1.342 (7)	C12–C11–C10–N2	180.0 (5)	C8–C7–C6	118.0 (5)
N1–C1	1.350 (5)	N3–C11–C10–C9	178.8 (4)	C18–C17–C16	119.3 (5)
N3–C15	1.336 (7)	C12–C11–C10–C9	-0.9 (8)	N2–C10–C9	120.3 (4)
N3–C11	1.359 (6)	C30–N6–C26–C27	-0.5 (7)	N2–C10–C11	114.1 (4)
N4–C16	1.332 (6)	NI1–N6–C26–C27	173.1 (4)	C9–C10–C11	125.6 (5)
N4–C20	1.365 (6)	C30–N6–C26–C25	-179.0 (4)	C23–C22–C21	117.7 (5)
N6–C30	1.325 (7)	NI1–N6–C26–C25	-5.4 (5)	C22–C23–C24	122.0 (5)
N6–C26	1.356 (5)	C26–N6–C30–C29	1.8 (8)	C22–C23–CL2	119.8 (4)
C6–C7	1.387 (6)	NI1–N6–C30–C29	-170.8 (4)	C24–C23–CL2	118.2 (4)
C6–C1	1.493 (6)	C16–N4–C20–C19	-0.8 (7)	N5–C21–C22	120.7 (5)
C11–C12	1.382 (7)	NI1–N4–C20–C19	177.2 (4)	C22–C21–C20	125.5 (5)
C11–C10	1.477 (7)	C16–N4–C20–C21	178.8 (4)	C8–C9–C10	117.6 (5)
N5–NI1–N2	178.92 (19)	NI1–N4–C20–C21	-3.3 (5)	N1–C5–C4	122.9 (5)
N5–NI1–N3	102.25 (15)	C21–N5–C25–C24	-0.4 (7)	C28–C27–C26	118.9 (5)
N2–NI1–N3	77.72 (16)	NI1–N5–C25–C24	178.2 (3)	C24–C25–C26	125.5 (5)
N5–NI1–N4	77.73 (16)	C21–N5–C25–C26	178.8 (4)		
N2–NI1–N4	101.20 (16)	NI1–N5–C25–C26	-2.6 (5)		
N3–NI1–N4	93.18 (13)	N6–C26–C25–N5	5.3 (6)	NI1–N4–C16–C17	-177.9 (4)
N3–NI1–N6	93.67 (16)	C27–C26–C25–N5	-173.2 (5)	N3–C11–C12–C13	0.2 (8)
N4–NI1–N6	155.63 (14)	N6–C26–C25–C24	-175.5 (4)	C10–C11–C12–C13	179.9 (5)
N5–NI1–N1	102.49 (15)	C27–C26–C25–C24	6.0 (8)	N4–C20–C19–C18	0.3 (7)
N2–NI1–N1	77.57 (16)	N6–C26–C27–C28	-1.0 (8)	C21–C20–C19–C18	-179.2 (5)
N3–NI1–N1	155.22 (14)	C25–C26–C27–C28	177.4 (5)	C5–C4–C3–C2	0.9 (9)
N4–NI1–N1	93.24 (16)	N6–C30–C29–C28	-1.7 (9)	N1–C1–C2–C3	-0.5 (7)
N6–NI1–N1	90.26 (13)	C20–N4–C16–C17	-0.2 (8)	C6–C1–C2–C3	176.7 (5)
C6–N2–C10	121.7 (3)	C20–C19	1.382 (7)	C4–C3–C2–C1	0.6 (8)
C6–N2–NI1	119.4 (3)	C20–C21	1.486 (7)	C11–N3–C15–C14	0.8 (8)
C10–N2–NI1	118.9 (3)	C25–C24	1.398 (6)	NI1–N3–C15–C14	-179.5 (4)
C25–N5–C21	122.0 (4)	C27–C28	1.381 (8)	C13–C14–C15–N3	-0.6 (8)
C25–N5–NI1	118.6 (3)	C8–C7	1.378 (7)	C30–C29–C28–C27	0.1 (9)
C21–N5–NI1	119.4 (3)	C8–C9	1.381 (7)	C26–C27–C28–C29	1.1 (8)
C5–N1–C1	118.0 (5)	C14–C13	1.368 (7)	C15–C14–C13–C12	0.2 (8)
C5–N1–NI1	127.0 (4)	C14–C15	1.390 (8)	C11–C12–C13–C14	0.0 (8)
C1–N1–NI1	114.9 (3)	C29–C28	1.360 (7)	C20–C19–C18–C17	1.1 (8)
C26–N6–NI1	114.0 (3)	C16–C17	1.379 (8)	N5–C25–C24–C23	1.3 (7)
N2–C6–C7	120.8 (4)	C12–C13	1.381 (7)	C26–C25–C24–C23	-177.8 (5)
N2–C6–C1	113.6 (4)	C19–C18	1.384 (7)	C9–C8–C7–C6	0.3 (7)
N3–C11–C12	121.4 (5)	C3–C2	1.390 (7)	CL1–C8–C7–C6	179.8 (3)
N3–C11–C10	114.3 (4)	C18–C17	1.368 (7)	N2–C6–C7–C8	1.3 (7)
C12–C11–C10	124.2 (4)	C24–C23	1.387 (7)	C1–C6–C7–C8	-177.6 (4)
				C19–C18–C17–C16	-2.0 (8)

N1–C1–C2	122.3 (4)	C22–C23	1.381 (7)	N4–C16–C17–C18	1.6 (8)
N1–C1–C6	114.4 (4)	C22–C21	1.380 (7)	C21–C22–C23–C24	-1.2 (7)
C2–C1–C6	123.2 (4)	C1–C2	1.387 (6)	C21–C22–C23–CL2	179.3 (3)
N6–C26–C27	121.3 (5)	C10–C9	1.399 (6)	C25–C24–C23–C22	-0.5 (7)
N6–C26–C25	114.8 (4)	C26–C27	1.385 (7)	C25–C24–C23–CL2	179.0 (3)
C27–C26–C25	123.9 (4)	C26–C25	1.471 (7)	C25–N5–C21–C22	-1.4 (7)
C3–C4–C5	118.5 (5)	C4–C3	1.373 (7)	NI1–N5–C21–C22	180.0 (3)
N6–C30–C29	123.1 (5)	C4–C5	1.384 (8)	C25–N5–C21–C20	-178.8 (4)
N5–C21–C20	113.7 (4)	C30–C29	1.386 (8)	NI1–N5–C21–C20	2.6 (5)
N4–C20–C19	122.1 (5)	C7–C8–C9	121.7 (4)	C23–C22–C21–N5	2.1 (7)
N4–C20–C21	114.2 (4)	C7–C8–CL1	118.8 (4)	C23–C22–C21–C20	179.2 (5)
C19–C20–C21	123.7 (4)	C9–C8–CL1	119.5 (4)	N4–C20–C21–N5	0.6 (6)
N5–C25–C24	120.1 (5)	C13–C14–C15	118.0 (5)	C19–C20–C21–N5	-179.9 (4)
N5–C25–C26	114.4 (4)	N5–NI1–N6	77.97 (16)	N4–C20–C21–C22	-176.7 (4)
C10–N2–C6–C7	-1.4 (7)	N2–NI1–N6	103.11 (15)	C19–C20–C21–C22	2.9 (7)
NI1–N2–C6–C7	177.0 (3)	C28–C29–C30	118.4 (5)	C7–C8–C9–C10	-1.7 (7)
C10–N2–C6–C1	177.6 (4)	N4–C16–C17	123.2 (5)	CL1–C8–C9–C10	178.8 (4)
NI1–N2–C6–C1	-4.0 (5)	C13–C12–C11	119.5 (5)	N2–C10–C9–C8	1.6 (7)
C15–N3–C11–C12	-0.6 (7)	C20–C19–C18	118.9 (5)	C11–C10–C9–C8	-177.5 (5)
NI1–N3–C11–C12	179.6 (4)	C4–C3–C2	119.7 (5)	C1–N1–C5–C4	2.8 (8)
C15–N3–C11–C10	179.7 (4)	C1–C2–C3	118.4 (5)	NI1–N1–C5–C4	-174.5 (5)
NI1–N3–C11–C10	-0.1 (5)	N3–C15–C14	123.5 (5)	C3–C4–C5–N1	-2.7 (9)
C5–N1–C1–C2	-1.2 (7)	C29–C28–C27	119.8 (6)		

TABLE-3
GEOMETRIC PARAMETERS FOR HYDROGEN BONDS AND
OTHER INTERMOLECULAR CONTACTS (Å, °) OPERATING
IN THE CRYSTAL STRUCTURE OF [Ni(Cltpy)$_2$]Cl$_2$·2H$_2$O

D–H···A	D-H	H···A	D···A	D–H···A
O1-H2O1···Cl3[i]	0.82	2.44	3.2587	174
O1-H1O1···Cl3[ii]	0.83	2.44	3.2079	154
O2-H2O2···Cl4	0.83	2.38	3.1875	165
O2-H1O2···Cl4[iii]	0.81	2.42	3.2204	170
C5-H5···Cl3[iv]	0.93	2.82	3.5266	134
C12-H12···O1[v]	0.93	2.58	3.4549	156
C13-H13···Cl3[vi]	0.93	2.81	3.6784	156
C15-H15···O2[vii]	0.93	2.58	3.2459	129
C19-H19···Cl3[viii]	0.93	2.67	3.5859	167
C30-H30···O1[iv]	0.93	2.54	3.2677	135

i: 1/2-x, -1/2+y, 1/2+z; ii: -x, 1-y, 1/2+z; iii: -1/2+x, 1/2-y, z; iv: 1/2+x, 1/2-y, z; v: 1+x, y, z; vi: 3/2-x, -1/2+y, 1/2+z; vii: 1-x, -y, 1/2+z; viii: 1+x, -1+y, z.

TABLE-4
CRYSTAL DATA AND STRUCTURE
REFINEMENT OF [Ni(Cltpy)$_2$]Cl$_2$·2H$_2$O

CCDC number	1914492
Empirical formula	C$_{30}$H$_{24}$N$_6$O$_2$Cl$_4$Ni
Formula weight	701.06
Temperature (K)	296.15
Crystal system	Orthorhombic
Space group	*Pna*2$_1$
a (Å)	10.2278(14)
b (Å)	16.388(2)
c (Å)	17.876(2)
Volume (Å^3)	2996.3(7)
Z	4
ρ$_{calc}$ (g/cm^3)	1.554
μ (mm^{-1})	1.045
F(000)	1432.0
Crystal size (mm^3)	0.35 × 0.35 × 0.3
Radiation	Mo*K*α (λ = 0.71073)
2θ range for data collection (°)	6.372 to 56.686
Index ranges	-13 ≤ h ≤ 12, -21 ≤ k ≤ 19, -23 ≤ l ≤ 20
Reflections collected	23112
Independent reflections	6486 [R$_{int}$ = 0.0566, R$_{sigma}$ = 0.0704]
Data/restraints/parameters	6486/5/411
Goodness-of-fit on F^2	0.922
Final R indexes [I>=2σ(I)]	R$_1$ = 0.0395, wR$_2$ = 0.0691
Final R indexes [all data]	R$_1$ = 0.0873, wR$_2$ = 0.0807
Largest diff. peak/hole (e Å^{-3})	0.25/-0.40
Flack parameter	0.166(17)

occupied by hydrophilic O–H···Cl$^-$ hydrogen bonded chains running down the crystallographic *a*-axis (Fig. 5). The crystal data and structural refinement details including CCDC number of the complex are given in Table-4.

Diffuse reflectance spectral studies: The DR spectrum of Ni(Cltpy)$_2$(Cl$_2$)·2H$_2$O recorded in the range 400-900 nm is shown in Fig. 6a. DR spectrum of Ni(Cltpy)$_2$(Cl$_2$)·2H$_2$O showed a major peak at 630 nm (diffuse reflectance 10%) as a result of transitions between valence and conduction bands. The band gap energy of the complex was obtained from DR spectrum by following Kubelka-Munk (K-M) theory [25]. Intercept of the tangent to the plot of [F(R$_\infty$)hν]$^{1/2}$ against photon energy hν is depicted in Fig. 6b. The calculation of K-M function F(R$_\infty$) and energy of photon (hν) was done by the following equations:

$$F(R_\infty) = \frac{(1-R_\infty)^2}{2R_\infty} \qquad (1)$$

$$h\nu = \frac{1240}{\lambda} \qquad (2)$$

where R$_\infty$ = reflection coefficient of sample, λ = the absorption wavelength. The band gap (E$_g$) energy of Ni(Cltpy)$_2$(Cl$_2$)·2H$_2$O was found to be 2.38 eV. The E$_g$ values not only depend on the preparation methods but also on the experimental conditions, which could either support or hamper the formation of structural defects. The development of these structural defects plays a key role in controlling the extent of structural order-disorder of the materials and hence, the number of intermediary energy
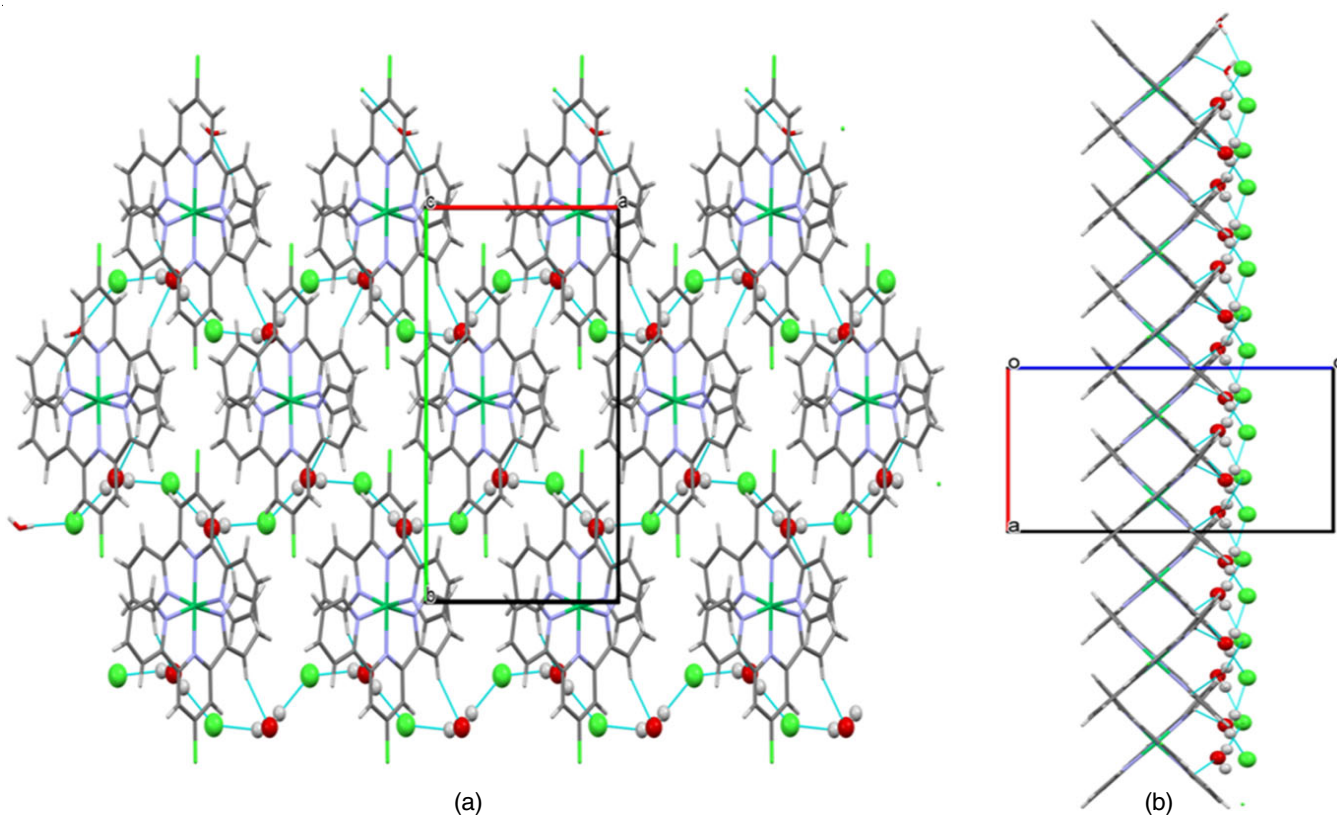
Fig. 4. (a) A partial view down the *c*-axis of the crystal packing of [Ni(Cltpy)₂]Cl₂·2H₂O displaying formation of two dimensional sheets along *ac*-plane, (b) Another view of the two dimensional sheet when viewed down *b*-axis
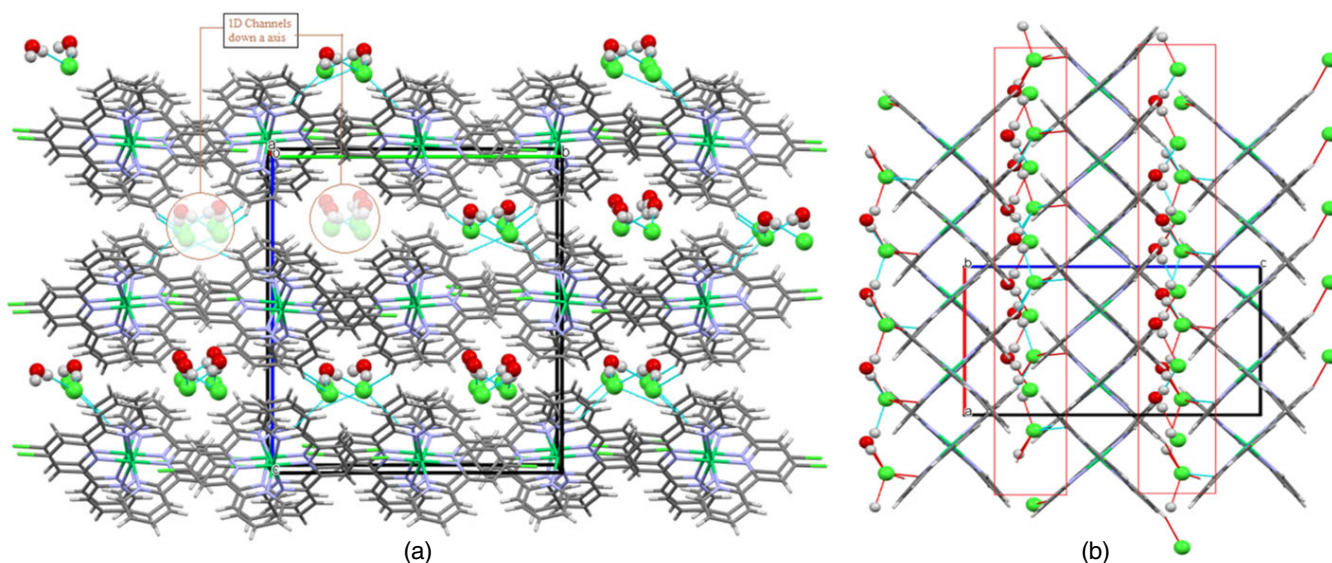

Fig. 5. (a) A partial view down approximate *a*-axis of the crystal packing of [Ni(Cltpy)₂]Cl₂·2H₂O displaying three dimensional network with channels running down *a*-axis, (b) Another view of the three dimensional network when viewed down *b*-axis

levels within the band gap. There are certain reports to substantiate the possibility of accomplishing smaller band gap with the incorporation of electron-donating substituents that can destabilize the HOMO and electron-withdrawing substituents in order to destabilize the LUMO on the ancillary ligand [26,27].

Photoluminescence studies: Excitation and emission spectra recorded at room temperature and internationale de l'eclairage (CIE) graph of Ni(Cltpy)₂(Cl₂)·2H₂O are depicted

in Fig. 7. The excitation spectrum of the complex (Fig. 7a) at 485 nm emission wavelength showed major excitations at 330, 344 and 383 nm, revealing that this phosphor could be effectively excited by UV LED chip. The emission spectrum (Fig. 7b) of the complex at excitation wavelength 383 nm exhibited an intense peak at 490 nm. The CIE 1931 chromaticity coordinates [28,29] were calculated at excitation wavelength 383 nm. The estimated CIE values for the possible excitation were
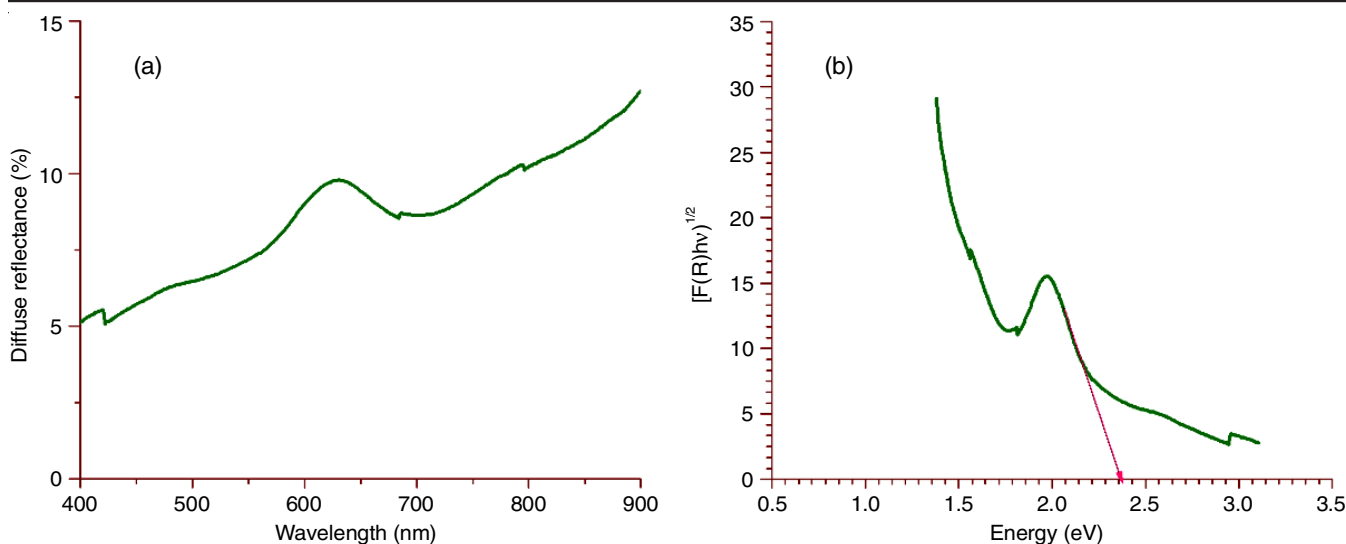
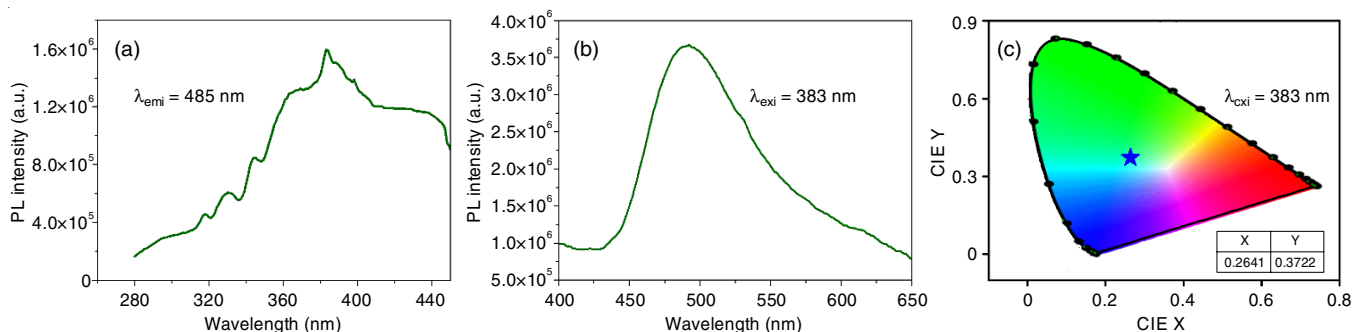Fig. 6. (a) DR spectrum, (b) plot of $[F(R_\infty)h\nu]^{1/2}$ *versus* energy of $[Ni(Cltpy)_2]Cl_2 \cdot 2H_2O$

Fig. 7. (a) PL excitation spectrum, (b) PL emission spectrum and (c) CIE graph of $[Ni(Cltpy)_2]Cl_2 \cdot 2H_2O$

tabulated and were inserted in the right corner of Fig. 7c. From the location of colour coordinates, one could observe that the emission colour of this material was blue green.

SEM studies: A study on surface morphology was undertaken by capturing the SEM images of $[Ni(Cltpy)_2]Cl_2 \cdot 2H_2O$ (Fig. 8), which revealed different surface morphology and arrangement of molecules. The SEM image revealed a rough surface topography, which clearly revealed non-uniformly dispersed shattered pieces on the surface of the material. The complexes, displaying identical morphologies and with different particle sizes, demonstrated efficient photoluminescent properties as reported earlier [30,31].
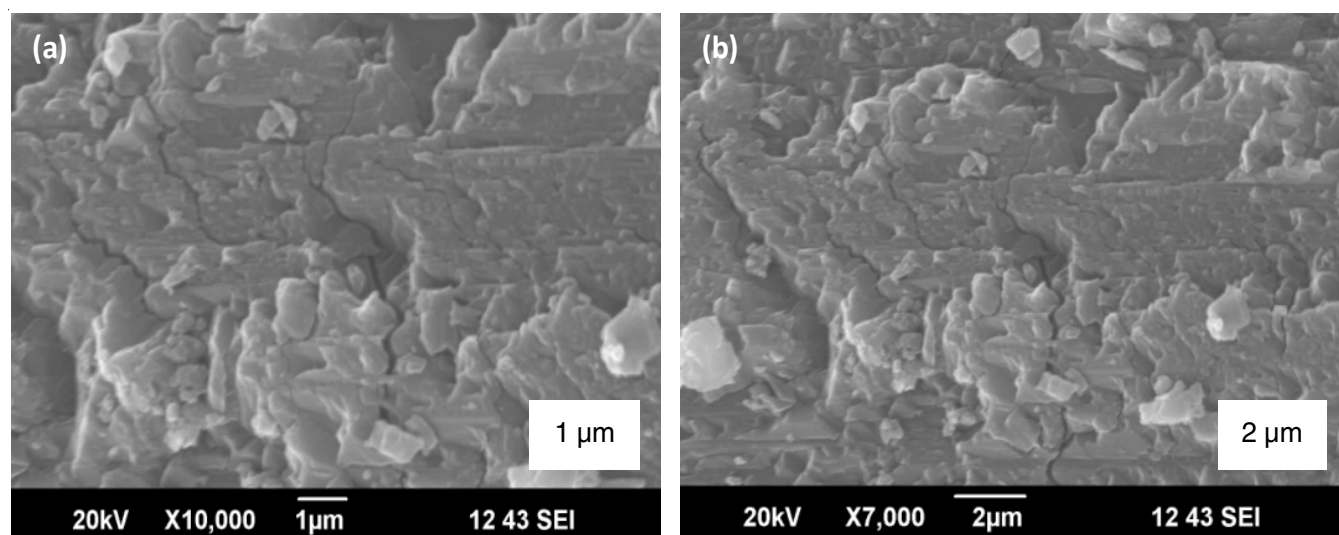

Fig. 8. Scanning electron microscope images of $[Ni(Cltpy)_2]Cl_2 \cdot 2H_2O$ (a) representing particle size with 1 μm scale, (b) representing particle size with 2 μm scale

Conclusion

The present study concluded that the nickel(II) complex, Ni(Cltpy)$_2$Cl$_2$·2H$_2$O, can be prepared through the direct interaction of a NiCl$_2$·6H$_2$O with the Cltpy chelating ligand in an alcohol medium. The synthesized nickel(II) complex gets crystallized in methanol-chloroform (1:9) solvent system. Crystal data revealed that the nickel(II) complex crystallizes in orthorhombic *Pna*2$_1$ space group with two molecules of solvent water molecule and two free chloride anions as counter ions. Simultaneous TG-DTA analysis confirmed the exhibition of reasonably good thermal stability by the complex, one of the important prerequisites for use in OLED devices, and good solubility of the complex in H$_2$O and in common organic solvents like C$_2$H$_5$OH, CH$_3$OH and DMSO could practically find itself suitable for the fabrication of a device known to display electroluminescence. The title complex displayed the emission of blue green light, in accordance with its CIE graph. The facile synthesis, achievement of good experimental yield and the subsequent investigation of photophysical properties through photoluminescence (PL) and diffuse reflectance (DR) spectra revealed that this phosphor could become efficient precursor in the fabrication of OLED devices.

CONFLICT OF INTEREST

The authors declare that there is no conflict of interests regarding the publication of this article.

REFERENCES

1. C.W. Tang and S.A. VanSlyke, *Appl. Phys. Lett.*, **51**, 913 (1987);
   https://doi.org/10.1063/1.98799
2. M.A. Baldo, D.F. O'Brien, Y. You, A. Shoustikov, S. Sibley, M.E. Thompson and S.R. Forrest, *Nature*, **395**, 151(1998);
   https://doi.org/10.1038/25954
3. S.A. Sapp, C.M. Elliott, C. Contado, S. Caramori and C.A. Bignozzi, *J. Am. Chem. Soc.*, **124**, 11215 (2002);
   https://doi.org/10.1021/ja027355y
4. W. Zhang, P. Liu, A. Sadollahkhani, Y. Li, B. Zhang, F. Zhang, M. Safdari, Y. Hao, Y. Hua and L. Kloo, *ACS Omega*, **2**, 9231 (2017);
   https://doi.org/10.1021/acsomega.7b01434
5. G. Li, M.D. Brady and G.J. Meyer, *J. Am. Chem. Soc.*, **140**, 5447 (2018);
   https://doi.org/10.1021/jacs.8b00944
6. M. Srinivas, T.O.S. Kumar, K.M. Mahadevan, S. Naveen, G.R. Vijayakumar, H. Nagabhushana, M.N. Kumara and N.K. Lokanath, *J. Sci. Adv. Mater. Devices*, **1**, 324 (2016);
   https://doi.org/10.1016/j.jsamd.2016.07.002
7. B.Z. Momeni, F. Rahimi, S.M. Jebraeil and J. Janczak, *J. Mol. Struct.*, **1150**, 196 (2017);
   https://doi.org/10.1016/j.molstruc.2017.08.081
8. K. Das, A. Datta, S. Roy, J.K. Clegg, E. Garribba, C. Sinha and H. Kara, *Polyhedron*, **78**, 62 (2014);
   https://doi.org/10.1016/j.poly.2014.04.032
9. A. Donmez, G. Oylumluoglu, M.B. Coban, C. Kocak, M. Aygun and H. Kara, *J. Mol. Struct.*, **1149**, 569 (2017);
   https://doi.org/10.1016/j.molstruc.2017.08.027
10. E. Gungor, M.B. Coban, H. Kara and Y. Acar, *J. Clust. Sci.*, **29**, 967 (2018);
    https://doi.org/10.1007/s10876-018-1406-2
11. D.A. Kara, A. Donmez, H. Kara, M.B. Coban, *Acta Crystallogr. C*, **74**, 901 (2018);
    https://doi.org/10.1107/S2053229618009166
12. X. Ren, B.D. Alleyne, P.I. Djurovich, C. Adachi, I. Tsyba, R. Bau and M.E. Thompson, *Inorg. Chem.*, **43**, 1697 (2004);
    https://doi.org/10.1021/ic035183f
13. L. He, X. Wang and L. Duan, *ACS Appl. Mater. Interface*, **10**, 11801 (2018);
    https://doi.org/10.1021/acsami.8b00466
14. A. Abedi, E. Saemian and V. Amani, *J. Struct. Chem.*, **56**, 1545 (2015);
    https://doi.org/10.1134/S0022476615080132
15. C. Bizzarri, E. Spuling, D.M. Knoll, D. Volz and S. Bräse, *Coord. Chem. Rev.*, **373**, 49 (2018);
    https://doi.org/10.1016/j.ccr.2017.09.011
16. H. Rudmann, S. Shimada and M.F. Rubner, *J. Am. Chem. Soc.*, **124**, 4918 (2002);
    https://doi.org/10.1021/ja012721j
17. Bruker APEX2, SAINT-Plus and SADABS. Bruker AXS Inc., Madison, Wisconsin, USA (2004).
18. G.M. Sheldrick, *Acta Crystallogr. A*, **71**, 3 (2015);
    https://doi.org/10.1107/S2053273314026370
19. L.J. Farrugia, *J. Appl. Cryst.*, **45**, 849 (2012);
    https://doi.org/10.1107/S0021889812029111
20. A.L. Spek, *Acta Crystallogr. D*, **65**, 148 (2009);
    https://doi.org/10.1107/S090744490804362X
21. C.F. Macrae, I.J. Bruno, J.A. Chisholm, P.R. Edgington, P. McCabe, E. Pidcock, L. Rodriguez-Monge, R. Taylor, J. van de Streek and P.A. Wood, *J. Appl. Cryst.*, **41**, 466 (2008);
    https://doi.org/10.1107/S0021889807067908
22. S. Arounaguiri, D. Easwaramoorthy, A. Ashokkumar, A. Dattagupta and B.G. Maiya, *Proc. Indian Acad. Sci. (Chem. Sci.)*, **112**, 1 (2000);
    https://doi.org/10.1007/BF02704295
23. D.C.-Sulikowska, A. Malinowska and J.R.-Doczekalska, *Polish J. Chem.*, **74**, 607 (2000).
24. S.K. Mishra and S.B. Kanungo, *J. Therm. Anal.Calorim.*, **38**, 2417 (1992);
    https://doi.org/10.1007/BF01974621
25. A.E. Morales, E.S. Mora and U. Pal, *Rev. Mex. Fisica*, **53**, 18 (2007).
26. L. He, J. Qiao, L. Duan, G.F. Dong, D.Q. Zhang, L.D. Wang and Y. Qiu, *Adv. Funct. Mater.*, **19**, 2950 (2009);
    https://doi.org/10.1002/adfm.200900723
27. R.D. Costa, F.J. Cespedes-Guirao, E. Ortí, H.J. Bolink, J. Gierschner, F. Fernández-Lazaro and A. Sastre-Santos, *Chem. Commun.*, **26**, 3886 (2009);
    https://doi.org/10.1039/b905367k
28. Publication CIE no. 17.4, International Lighting Vocabulary, Central Bureau of the Commission Internationale de L 'Eclairage, Vienna, Austria (1987).
29. Publication CIE no. 15.2, Colorimetry, Central Bureau of the Commission Internationale de L 'Eclairage, Edn. 2, Vienna, Austria (1986).
30. R. Lakshmanan, N.C. Shivaprakash and S. S. Nair, *J. Lumin.*, **168**, 145 (2015);
    https://doi.org/10.1016/j.jlumin.2015.08.005
31. V. Kumar, M. Gohain, J.H. Van Tonder, B.C.B. Bezuindenhoudt, S. Ponra, O.M. Ntwaeaborwa and H.C. Swart, *Opt. Mater.*, **50B**, 275 (2015);
    https://doi.org/10.1016/j.optmat.2015.11.009